


In vivo Imaging of Reis–Bücklers and Thiel–Behnke Corneal Dystrophies Using Anterior Segment Optical Coherence Tomography

This article was published in the following Dove Press journal:
Clinical Ophthalmology

Tsubasa Nishino
Akira Kobayashi
Natsuko Mori 
Hideaki Yokogawa
Kazuhisa Sugiyama

Department of Ophthalmology,
Kanazawa University Graduate School of
Medical Science, Kanazawa, Japan

Purpose: To investigate in vivo corneal changes of genetically confirmed Reis–Bücklers corneal dystrophy (RBCD) and Thiel–Behnke corneal dystrophy (TBCD) using anterior segment optical coherence tomography (AS-OCT).

Design: A single-center, prospective, comparative case series.

Methods: Seven patients from 3 pedigrees (3 males, 4 females) with RBCD [Arg124Leu (R124L) heterozygous missense mutation of human transforming growth factor beta-induced (*TGFBI*) gene] and 4 patients from 3 pedigrees (3 males, 1 female) with TBCD [Arg555Gln (R555Q) heterozygous missense mutation of *TGFBI* gene] were examined. Six patients with RBCD and three patients with TBCD exhibited recurrence after corneal surgery including penetrating keratoplasty, phototherapeutic keratectomy, and electrolysis. All patients were examined by slit-lamp biomicroscopy followed by AS-OCT. Selected AS-OCT images of the cornea were evaluated qualitatively for changes in shape and degree of light reflection of corneal deposits.

Results: Slit-lamp biomicroscopy showed characteristic irregular gray opacities in Bowman's layer in each dystrophy: a geographic pattern in RBCD and a honeycomb pattern in TBCD. In each dystrophy, distinct characteristic deposits were observed by AS-OCT as a banding lesion in Bowman's layer and its adjacent epithelium/stroma. In RBCD, the banding lesion was highly reflective and sharply margined at the stroma. In contrast, deposits in TBCD in the same layer showed a saw-tooth pattern toward the epithelium and poorly margined at the stroma.

Conclusion: AS-OCT is able to clearly identify characteristic in vivo corneal microstructural changes associated with RBCD and TBCD. As a result, in vivo differentiation of RBCD and TBCD can be achieved.

Keywords: Reis–Bücklers corneal dystrophy, Thiel–Behnke corneal dystrophy, anterior segment optical coherence tomography, genetic mutational analysis, human transforming growth factor beta-induced gene, *TGFBI*

Introduction

The Bowman's layer is a smooth, non-regenerating, acellular layer located between the superficial epithelium and the stroma in the cornea.¹ To date, two distinct types of corneal dystrophies that mainly affect Bowman's layer have been recognized: Reis–Bücklers corneal dystrophy (RBCD) and Thiel–Behnke corneal dystrophy (TBCD).^{2–5} RBCD is a bilateral and autosomal dominant inherited disease that develops early in childhood; it is also characterized by recurrent painful erosions, corneal opacities in a geographic pattern in Bowman's layer, and a progressive

Correspondence: Akira Kobayashi
Department of Ophthalmology, Kanazawa
University Graduate School of Medical
Science, 13-1 Takara-Machi, Kanazawa-shi,
Ishikawa-ken 920-8641, Japan
Tel +81-76-265-2403
Fax +81-76-222-9660
Email eyekoba@gmail.com

decrease of visual acuity.^{2,3} Similar to RBCD, TBCD, or honeycomb corneal dystrophy,⁴ is an autosomal dominant corneal dystrophy of Bowman's layer that has a characteristic, bilateral, honeycomb arrangement of sub-epithelial corneal opacities which appear between the ages of 10–20 years. It also presents with frequently recurrent epithelial erosions. Genetic analysis has revealed that the dystrophies are caused by different mutations of the same gene, human transforming growth factor beta-induced gene (*TGFBI*).⁵ RBCD is caused by Arg124Leu (R124L) heterozygous missense mutation of the *TGFBI* gene, and TBCD is caused by an Arg555Gln (R555Q) heterozygous missense mutation.^{6,7} The International Committee for Classification of Corneal Dystrophies (IC3D) has recently categorized these dystrophies as “epithelial–stromal *TGFBI* dystrophies”.⁸

Recent advances in imaging device technology in the corneal research and clinical fields enable in vivo analysis of the cornea. Both in vivo laser confocal microscopy (IVCM) and anterior segment optical coherence tomography (AS-OCT) are useful for clinical diagnosis and following the clinical course of corneal diseases.^{9–20} We have previously characterized in vivo histology of these dystrophies and reported the usefulness of IVCM in differential diagnosis of these dystrophies.⁹ AS-OCT allows contactless and less invasive corneal imaging in real time from the epithelium to the endothelium in vivo. For now, only a few case series have been reported using AS-OCT on patients with RBCD and TBCD independently.^{15–17} In this study, we investigate in vivo characteristics of the cornea using high-resolution AS-OCT in patients with genetically confirmed RBCD and TBCD to determine the usefulness of the AS-OCT in differentiating these two dystrophies.

Materials and Methods

This single-center prospective research plan was approved by the Medical Ethics Committee of Kanazawa University (approval number: 2720), and human patient sample collection strictly followed the Association for Research in Vision and Ophthalmology (ARVO) statement on human subjects and the ethical principles of the Declaration of Helsinki. Written informed consent was obtained from all participants before enrollment into this study.

Seven patients from 3 pedigrees (3 males, 4 females) with RBCD and 4 patients from 3 pedigrees (3 males, 1 female) with TBCD were examined. The patients were first examined and photographed with slit-lamp biomicroscopy.

Then, AS-OCT (RTVue-100 Optovue Inc, Fremont, California, USA) was performed followed by blood sample collection which was tested for genetic mutational analysis using polymerase chain reaction (PCR) upon written informed consent. Selected high-quality AS-OCT images of the cornea with scan quality index more than 60 were evaluated qualitatively for changes in the shape and degree of light reflection. Genetic mutation analysis of the *TGFBI* gene was performed on all patients enrolled.

Anterior Segment Optical Coherence Tomography (AS-OCT)

All patients were examined using AS-OCT with a corneal adaptor module. This system captures 26,000 A-scans per second and has a laser diode of 840nm and an axial resolution of 5μm. Line images obtained by the AS-OCT were used in this study. All images were acquired by an experienced examiner. Images were evaluated with special attention to changes in the degree of the reflectivity of each corneal layer.

Results

Genetic mutational analysis by PCR confirmed a R124L heterozygous missense mutation of the *TGFBI* gene in all RBCD patients, and a R555Q heterozygous missense mutation of the *TGFBI* gene in all TBCD patients (Table 1). Table 1 summarizes demographic data, history of corneal surgery, and AS-OCT findings of all patients. Six patients with RBCD and three patients with TBCD exhibited recurrence after corneal surgery including penetrating keratoplasty (PK), phototherapeutic keratectomy (PTK), and electrolysis.²¹ The examiner was masked as to the clinical and genetic status of the source of the images.

Slit-Lamp Biomicroscopy

In the patients with RBCD, slit-lamp biomicroscopy revealed bilateral, gray, amorphous, geographic opacities of various sizes in Bowman's layer of the central and mid-peripheral cornea (Figure 1A and B). In the peripheral cornea, opacities were separated from the limbus by a clear zone. In cases that had undergone PK (cases 1, 3, and 6), a similar geographic opacity was observed on the host as well as the grafted corneas at Bowman's layer (Figure 1C). In the recurrent case after PTK and electrolysis (case 4), a similar geographic opacity was observed in Bowman's layer (Figure 1D). Fluorescein staining was

Table 1 Clinical and AS-OCT Findings of Bowman's Layer Dystrophies (Epithelial–Stromal *TGFBI* Dystrophies)

Patient	Pedigree	Age/ Sex (Years)	Diagnosis	<i>TGFBI</i> Mutation	BCVA (OD/ OS)	History of Corneal Surgery	AS-OCT Findings of Bowman's Layer**
1	I (proband)	46/F	RBCD	Arg124Leu	0.4/0.7	PK (OU)	Highly reflective banding lesion (host: thick, donor: thin)
2	I (daughter of patient 1)	8/F	RBCD	Arg124Leu	0.6/0.9	None	Highly reflective thin banding lesion
3	2 (proband)	72/F	RBCD	Arg124Leu	0.1/0.2	PK, PTK, Electrolysis (OU)	Highly reflective thick banding lesion
4	2 (daughter of patient 3)	50/F	RBCD	Arg124Leu	0.6/0.8	PTK, Electrolysis (OU)	Highly reflective thick banding lesion
5	2 (grandson of patient 3)	15/M	RBCD	Arg124Leu	1.0/1.0	Electrolysis (OU)	Highly reflective thick banding lesion
6	3 (proband)	58/M	RBCD	Arg124Leu	0.03/0.5	PK, Electrolysis (OU)	Highly reflective thick banding lesion
7	3 (son of patient 6)	26/M	RBCD	Arg124Leu	1.0/1.0	Electrolysis (OU)	Highly reflective thick banding lesion
8	4 (proband)	70/M	TBCD	Arg555Gln	0.5/0.3	PTK (OS)	Moderately highly reflective thick banding lesion with saw-tooth pattern toward epithelium
9	4 (daughter of patient 8)	44/F	TBCD	Arg555Gln	0.5/0.7	None	Moderately highly reflective thick banding lesion with saw-tooth pattern toward epithelium
10	5	65/M	TBCD	Arg555Gln	0.4/1.0	PK (OS)	Moderately highly reflective thick banding lesion with saw-tooth pattern toward epithelium
11	6	44/M	TBCD	Arg555Gln	0.15/0.5	LKP, DALK, PK (OS)	Moderately highly reflective thick banding lesion with saw-tooth pattern toward epithelium (OD and host OS), normal in donor (OS)

Note: **Epithelium, stroma and endothelium were normal as observed by AS-OCT in all patients.

Abbreviations: RBCD, Reis–Bücklers corneal dystrophy; TBCD, Thiel–Behne corneal dystrophy; F, female; M, male; FBS, foreign body sensation; BCVA, best-corrected visual acuity; OD, oculus dexter; OS, oculus sinister.

negative in all cases. The deep stroma, Descemet's membrane, and endothelium presented as normal.

In cases with TBCD, honeycomb-shaped gray opacities were observed in Bowman's layer (Figure 2A–C). The opacities were located near the central cornea. In the cases that had undergone PK (cases 10 and 11), the similar weak honeycomb-shaped opacities were observed on the host and grafted corneas at Bowman's layer. The corneal epithelium, deep stroma, Descemet's membrane, and endothelium presented as normal. Fluorescein staining was negative in all patients.

Anterior Segment Optical Coherence Tomography (AS-OCT)

Table 1 summarizes in vivo AS-OCT findings for all patients enrolled in this study. In patients with RBCD who had not undergone PK (cases 2, 4, and 5), distinct characteristic deposits were observed as a highly reflective, continuous, and sharply margined thin/thick band in Bowman's layer, adjacent epithelium, and stroma (Figure 3A and B). The band

lesion became thinner in the periphery and disappeared at the corneal limbus. Recurrence of the geographic lesion after PK was observed as a highly reflective thin band in Bowman's layer (Figure 3C). Recurrence of the geographic lesion after PTK and electrolysis presented as a highly reflective band with some irregularities in Bowman's layer (Figure 3D).

In contrast, deposits in the cornea of TBCD patients in Bowman's layer were moderately reflective, continuous, and poorly margined in the stroma (Figure 4A–C). The deposits showed a thick band in Bowman's layer and a saw-tooth pattern toward the corneal epithelium. The thickness of this band lesion was almost the same between the central and peripheral cornea. The lesion in TBCD was much less reflective compared with that in RBCD, and less distinct in the adjacent stroma. Corneal surface irregularities were not observed by AS-OCT.

In both dystrophies, the deep stromal layer was clear without any abnormal deposits, and Descemet's membrane and endothelial layer was also unremarkable in all eleven patients.

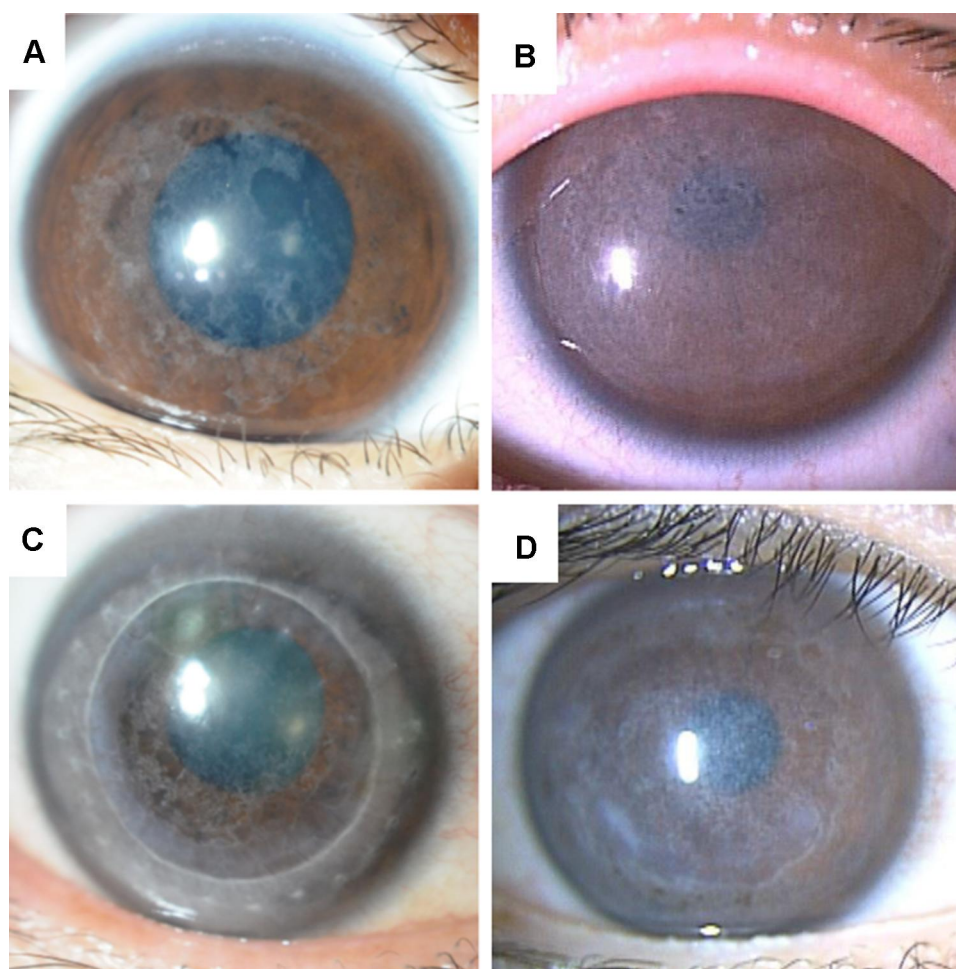


Figure 1 Slit-lamp biomicroscopy images of RBCD patients. **(A)** Slit-lamp biomicroscopy in the right eye of case 2 (8-year-old female) demonstrating gray, amorphous, geographic opacities of various sizes in Bowman's layer in the central and mid-peripheral cornea. **(B)** Slit-lamp biomicroscopy in the right eye of case 5 (15-year-old male), demonstrating gray confluent opacities in Bowman's layer in the central and mid-peripheral cornea. **(C)** Recurrence of RBCD after penetrating keratoplasty in the right eye of case 1. A similar geographic opacity was observed on the host and grafted corneas in Bowman's layer. **(D)** Recurrence of RBCD after phototherapeutic keratectomy and electrolysis in the right eye of case 4. A similar geographic opacity recurred in Bowman's layer.

Discussion

Herein, we demonstrated *in vivo* microstructural characteristics of the cornea in genetically confirmed RBCD and TBCD cases using high-resolution AS-OCT. Distinct characteristic AS-OCT findings were observed: a highly reflective, clearly margined band in Bowman's layer in RBCD, and a moderately reflective, poorly margined lesion with saw-tooth pattern toward the corneal epithelium in Bowman's layer in TBCD. These characteristics were also consistent in the recurrent corneal graft. Previously, a few case studies used AS-OCT to describe the corneal changes in RBCD and TBCD independently.^{15–17} However, there has not been a prospective comparative study using an identical device. We are unable to find any references concerning the comparison of high-quality AS-OCT findings of these Bowman's layer dystrophies through a PubMed search (as of

2019 August 4). Therefore, we are now certain that AS-OCT has been proven quite useful in differential diagnosis of RBCD and TBCD *in vivo* in real time.

In clinical practice, it has been challenging to distinguish between RBCD and TBCD,^{1–5} since the corneal appearance of these dystrophies looks quite similar, and most ophthalmologists are not familiar with these rare diseases. Histologically, RBCD shows the absence of Bowman's layer and granular dystrophy-type Masson-positive materials widely dispersed in thin bands beneath the epithelium, above and below what remains of Bowman's layer.²² On the other hand, TBCD shows the presence of a thick band of variable thickness consisting of hyaline, avascular, paucicellular connective tissue beneath the epithelium, which largely obliterates Bowman's layer.²² These histological characteristics are quite consistent with those images obtained by AS-OCT in

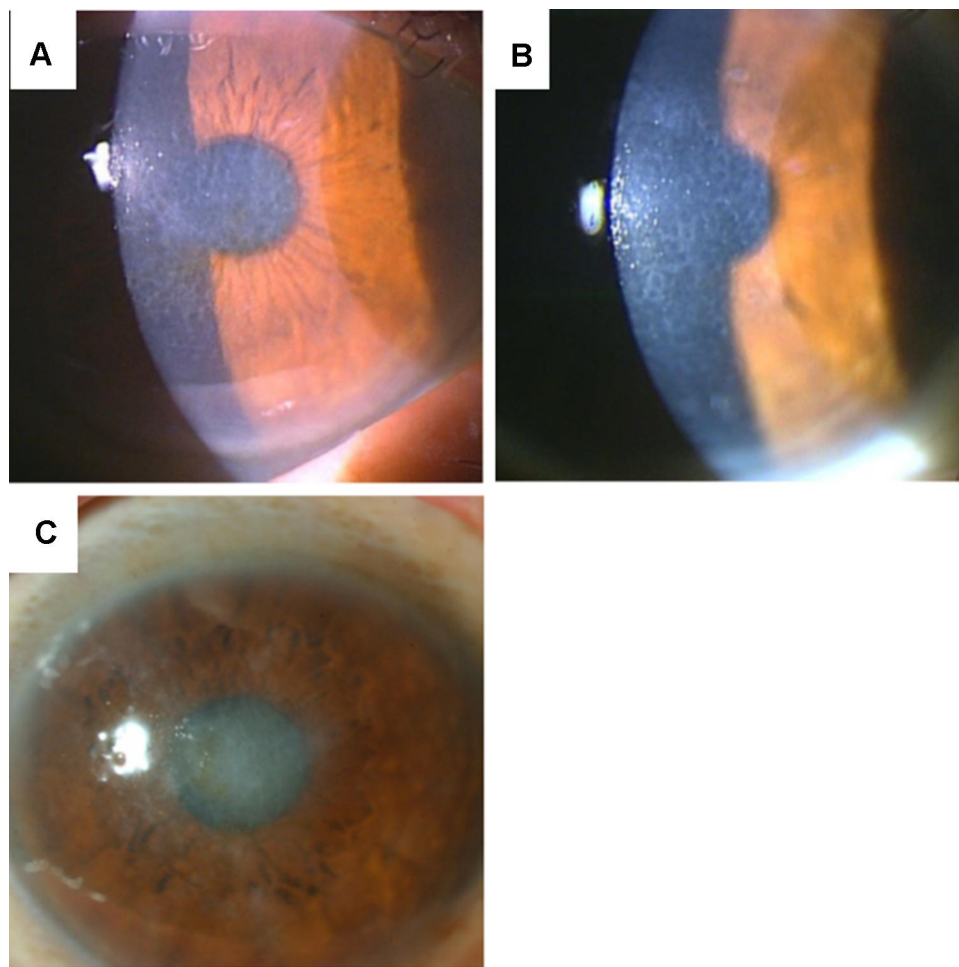


Figure 2 Slit-lamp biomicroscopy images of TBCD patients. (A) Slit-lamp biomicroscopy in the right eye of patient 8 revealed honeycomb-shaped gray opacities in Bowman's layer. (B) Slit-lamp biomicroscopy in the right eye of patient 9 revealed honeycomb-shaped gray opacities in Bowman's layer. (C) Slit-lamp biomicroscopy in the right eye of patient 11 revealed honeycomb-shaped gray opacities in Bowman's layer.

both dystrophies. Historically, electron microscopy has been used as a diagnostic tool for these dystrophies; RBCD shows numerous electron-dense rod-shaped deposits in the epithelial and Bowman's layer, and TBCD shows fibrous material appearing as twisted "curly fibers" measuring 9 to 10 nm in diameter.²² The advancement of molecular biology techniques enabled precise differential diagnosis of these dystrophies: RBCD is caused by an R124L mutation of the *TGFBI* gene and TBCD is caused by an R555Q mutation of the *TGFBI* gene.^{5,6}

We have previously reported that IVCM is able to distinguish these dystrophies. The deposits in Bowman's layer in RBCD showed high reflectivity of small granular materials without any shadows, and the deposits in Bowman's layer in TBCD showed homogeneous reflectivity with round-shaped edges accompanying dark shadows.⁹ High reflectivity of the deposits in RBCD and

moderate reflectivity of the deposits in TBCD observed by IVCM were consistent with the results obtained by AS-OCT in this study. However, "en face" IVCM images of granular materials without any shadows in RBCD and round-shaped edges accompanying dark shadows in TBCD were not evident by cross-section images obtained by AS-OCT. Further development of en face AS-OCT technology and/or increased resolution of AS-OCT may enable the collection of histology-like images with this device. Currently, volumetric imaging technique is improved in Fourier-domain full-field optical coherence tomography (FD-FF-OCT). Therefore, using FD-FF-OCT, high-resolution, high-speed, non-contact corneal volumetric imaging in vivo can be acquired.²³ The acquired images may reveal corneal microstructures, such as epithelium, stroma and endothelium, as well as subbasal nerves in these dystrophies.

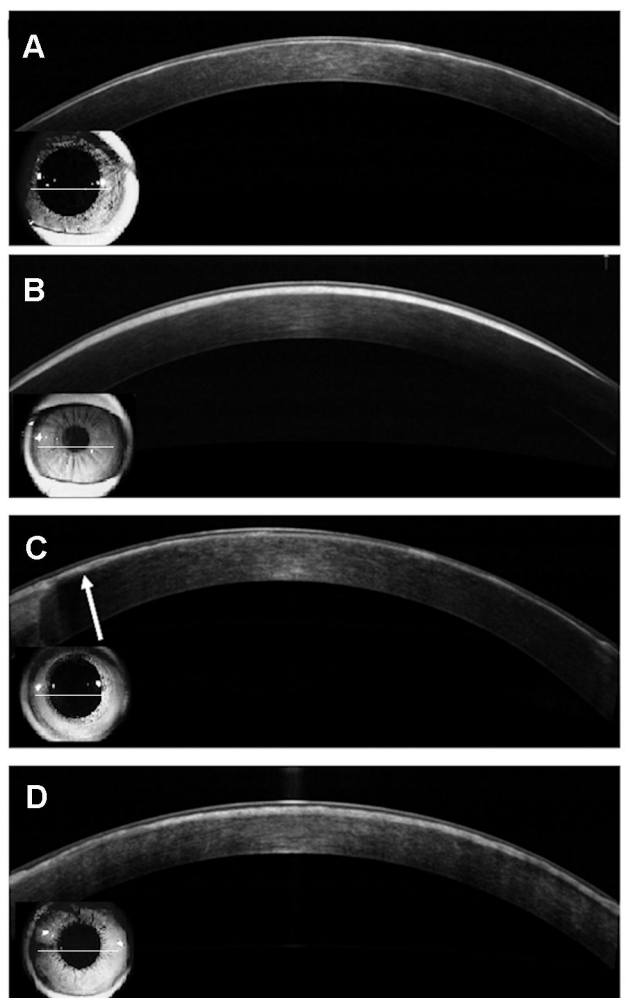


Figure 3 AS-OCT images of the cornea in patients with RBCD. Bar=250 μ m. Field of view caption is indicated at the lower left of each figures. **(A)** AS-OCT images of the right eye of case 2 showed a highly reflective, continuous, and sharply margined thin band in Bowman's layer. **(B)** AS-OCT images of the cornea of the right eye of case 5 showed a highly reflective, continuous, and sharply margined thick band in Bowman's layer. The band lesion became thinner in the periphery and disappeared before meeting the corneal limbus. **(C)** Recurrence of the geographic lesion after penetrating keratoplasty in case 1 was observed as a highly reflective thin band in Bowman's layer (arrow). **(D)** Recurrence of the geographic lesion after phototherapeutic keratectomy and electrolysis in the right eye of case 4 showed a highly reflective band with some irregularities in Bowman's layer.

Estimating the depth of opacities or morphological changes in corneal dystrophy cases is of paramount importance for choosing treatment options. Currently, several surgical options are available to treat Bowman's layer dystrophies: PTK, PK, deep anterior lamellar keratoplasty (DALK), and electrolysis. Clinical manifestation of TBCD is usually not severe, therefore, alleviating painful episodes due to corneal epithelial erosion may be enough. However, the corneal lesion of RBCD sometimes causes a severe decrease of visual acuity as well as eye pain. We prefer to choose electrolysis for patients of RBCD when the corneal dystrophy is not so severe, since it does not alter corneal refraction.²¹ Electrolysis is quite

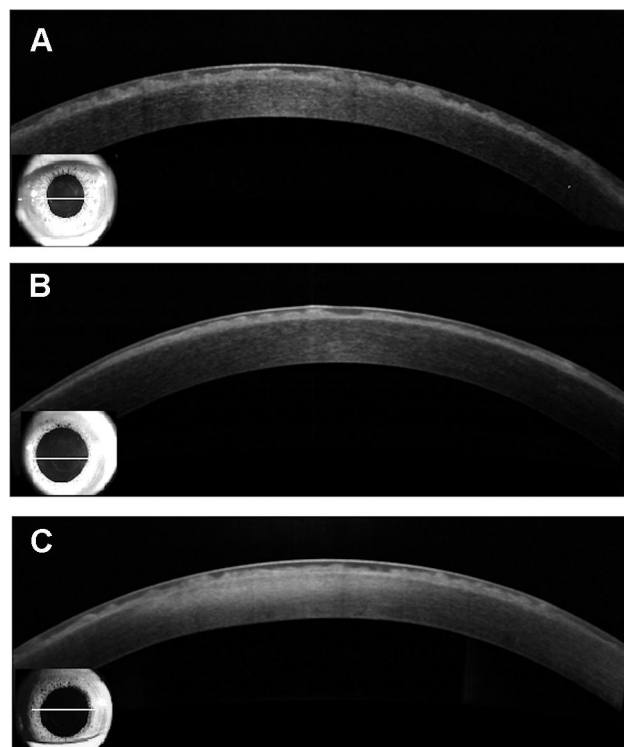


Figure 4 AS-OCT images of the cornea in patients with TBCD. Bar=250 μ m. Field of view caption is indicated at the lower left of each figures. **(A)** AS-OCT images of the cornea in the right eye of case 8 showed a moderately reflective, thick-banded lesion with a saw-tooth pattern toward the corneal epithelium in Bowman's layer. **(B)** AS-OCT images of the cornea in the right eye of case 9 showed a similar presentation as case 8. **(C)** AS-OCT images of the cornea in the right eye of case 11 showed a similar presentation as case 8.

effective to improve the visual acuity without refractive changes that are seen with PTK.²¹ However, severe and long-standing cases of RBCD like case 1 in this study may require PTK and/or PK, since the subepithelial opacities can progress deeper into the stroma. In this situation, AS-OCT may be useful to precisely measure the depth of the lesion to help choose a proper treatment option.

In conclusion, AS-OCT is able to clearly identify characteristic in vivo corneal microstructural changes associated with RBCD and TBCD with high resolution, and it could help in differentiation of RBCD and TBCD. In addition, this device may also be valuable for further research into corneal dystrophies, especially to elucidate the pathogenesis and natural course of these Bowman's layer dystrophies and other similar corneal dystrophies.

Meeting Presentation

The abstract of this paper was presented at the ARVO 2019 Annual Meeting as an abstract presentation with interim findings. The poster's abstract was published in

Investigative Ophthalmology & Visual Science, July 2019, Vol.60, 2103.

Funding

There is no funding to report.

Disclosure

No authors have any financial/conflicting interests to disclose for any of the products mentioned in this article. The authors report no conflicts of interest for this work.

References

- Kobayashi A, Yokogawa H, Sugiyama K. In vivo laser confocal microscopy of Bowman's layer of the cornea. *Ophthalmology*. 2006;113(12):2203–2208. doi:10.1016/j.ophtha.2006.05.058
- Reis W. Familiäre, fleckige Hornhautentartung [Familial fleck corneal change]. *Deutsch Med Wochenschr*. 1917;43:575.
- Bücklers M. Über eine weitere familiäre Hornhautdystrophie (Reis) [About a further familial corneal dystrophy (Reis)]. *Klin Monatsbl Augenheilkd*. 1949;114:386–397.
- Thiel HJ, Behnke H. A hitherto unknown subepithelial hereditary corneal dystrophy. *Klin Monatsbl Augenheilkd*. 1967;150(6):862–874.
- Küchle M, Green WR, Völcker HE, Barraquer J. Reevaluation of corneal dystrophies of Bowman's layer and the anterior stroma (Reis-Bücklers and Thiel-Behnke types): a light and electron microscopic study of eight corneas and a review of the literature. *Cornea*. 1995;14(4):333–354. doi:10.1097/00003226-199507000-00001
- Munier FL, Korvatska E, Djemai A, et al. Kerato-epithelin mutations in four 5q31-linked corneal dystrophies. *Nat Genet*. 1997;15(3):247–251. doi:10.1038/ng0397-247
- Okada M, Yamamoto S, Tsujikawa M, et al. Two distinct kerato-epithelin mutations in Reis-Bücklers corneal dystrophy. *Am J Ophthalmol*. 1998;126(4):535–542. doi:10.1016/S0002-9394(98)00135-4
- Weiss JS, Möller HU, Aldave AJ, et al. IC3D classification of corneal dystrophies – edition 2. *Cornea*. 2015;34(2):117–159. doi:10.1097/ICO.0000000000000307
- Kobayashi A, Sugiyama K. In vivo laser confocal microscopy findings for Bowman's layer dystrophies (Thiel-Behnke and Reis-Bücklers corneal dystrophies). *Ophthalmology*. 2007;114(1):69–75. doi:10.1016/j.ophtha.2006.05.076
- Kobayashi A, Fujiki K, Murakami A, Sugiyama K. In vivo laser confocal microscopy findings and mutational analysis for Schnyder's crystalline corneal dystrophy. *Ophthalmology*. 2009;116(6):1029–1037. doi:10.1016/j.ophtha.2008.12.042
- Cavanagh HD, Petroll WM, Alizadeh H, et al. Clinical and diagnostic use of in vivo confocal microscopy in patients with corneal disease. *Ophthalmology*. 1993;100(10):1444–1454. doi:10.1016/S0161-6420(93)31457-0
- Kaufman SC, Musch DC, Belin MW, et al. Confocal microscopy. A report by the American Academy of Ophthalmology. *Ophthalmology*. 2004;111(2):396–406. doi:10.1016/j.ophtha.2003.12.002
- Kobayashi A, Sugiyama K, Huang AJ. In vivo confocal microscopy in patients with central cloudy dystrophy of Francois. *Arch Ophthalmol*. 2004;122(11):1676–1679. doi:10.1001/archophth.122.11.1676
- Kobayashi A, Sakurai M, Shirao Y, et al. In vivo confocal microscopy and genotyping of a family with Thiel-Behnke (honeycomb) corneal dystrophy. *Arch Ophthalmol*. 2003;121(10):1498–1499. doi:10.1001/archophth.121.10.1498
- Siebelmann S, Scholz P, Sonnenschein S, et al. Anterior segment optical coherence tomography for the diagnosis of corneal dystrophies according to the IC3D classification. *Surv Ophthalmol*. 2018;63(3):365–380. doi:10.1016/j.survophthal.2017.08.001
- Liang Q, Pan Z, Sun X, et al. Reis-Bücklers corneal dystrophy: a reappraisal using in vivo and ex vivo imaging techniques. *Ophthalmic Res*. 2014;51(4):187–195. doi:10.1159/000358805
- Vajzovic LM, Karp CL, Haft P, et al. Ultra high-resolution anterior segment optical coherence tomography in the evaluation of anterior corneal dystrophies and degenerations. *Ophthalmology*. 2011;118(7):1291–1296. doi:10.1016/j.ophtha.2010.12.015
- Shukla AN, Cruzat A, Hamrah P. Confocal microscopy of corneal dystrophies. *Semin Ophthalmol*. 2012;27(5–6):107–116. doi:10.3109/08820538.2012.707276
- Nishino T, Kobayashi A, Mori N, et al. In vivo histology and p.L132V mutation in *KRT12* gene in Japanese patients with Meesmann corneal dystrophy. *Jpn J Ophthalmol*. 2019;63(1):46–55. doi:10.1007/s10384-018-00643-6
- Iovino C, Fossarello M, Giannaccare G, et al. Corneal endothelium features in Fuchs' endothelial corneal dystrophy: a preliminary 3D anterior segment optical coherence tomography study. *PLoS One*. 2018;13:207891.
- Mashima Y, Kawai M, Yamada M. Corneal electrolysis for recurrence of corneal stromal dystrophy after keratoplasty. *Br J Ophthalmol*. 2002;86(3):273–275. doi:10.1136/bjo.86.3.273
- Ridgway AE, Akhtar S, Munier FL, et al. Ultrastructural and molecular analysis of Bowman's layer corneal dystrophies: an epithelial origin? *Invest Ophthalmol Vis Sci*. 2000;41(11):3286–3292.
- Auksorius E, Borycki D, Stremplewski P, et al. In vivo imaging of the human cornea with high-speed and high-resolution Fourier-domain full-field optical coherence tomography. *Biomed Opt Express*. 2020;11(5):2849–2865. doi:10.1364/BOE.393801

Clinical Ophthalmology

Publish your work in this journal

Clinical Ophthalmology is an international, peer-reviewed journal covering all subspecialties within ophthalmology. Key topics include: Optometry; Visual science; Pharmacology and drug therapy in eye diseases; Basic Sciences; Primary and Secondary eye care; Patient Safety and Quality of Care Improvements. This journal is indexed on PubMed

Submit your manuscript here: <https://www.dovepress.com/clinical-ophthalmology-journal>

Dovepress

Central and CAS, and is the official journal of The Society of Clinical Ophthalmology (SCO). The manuscript management system is completely online and includes a very quick and fair peer-review system, which is all easy to use. Visit <http://www.dovepress.com/testimonials.php> to read real quotes from published authors.